CC10 at O (alpha-s): QCD corrections to e+ e- ---> mu- anti-muon-neutrino u anti-d at LEP-2 and the Next Linear Collider.

(Article begins on next page)

02 May 2024

ELSEVIER

QCD corrections to $e^+e^- \to \mu^-\bar{\nu}_\mu u \bar{d}$ at LEP2 and the Next Linear Collider: CC10 at $O(\alpha_s)$ [*]

Ezio Maina [a,1], Roberto Pittau [b,2], Marco Pizzio [a,3]

[a] *Dip. di Fisica Teorica, Università di Torino and INFN, Sezione di Torino, v. Giuria 1, 10125 Torino, Italy*
[b] *Paul Scherrer Institute, CH-5232 Villigen-PSI, Switzerland*

Abstract

QCD one-loop corrections to the semileptonic process $e^+e^- \to \mu^-\bar{\nu}_\mu u \bar{d}$ are computed. We compare the exact calculation with a "naive"approach to strong radiative corrections which has been widely used in the literature and discuss the phenomenological relevance of QCD contributions for LEP2 and NLC physics.

1. Introduction

The measurement of W-pair production at LEP2 will provide two additional pieces of information to our understanding of the Standard Model (SM) [1]. First, it will improve the determination of the W mass; second, it will probe the structure of triple gauge-boson couplings (TGC's). The mass of the W boson in the SM is tightly constrained. In fact an indirect determination of M_W can be obtained from a global fit of all electroweak data. The fit gives

$$M_W = 80.359 \pm 0.051^{+0.013}_{-0.024} \text{ GeV} \qquad (1)$$

where the central value correspond to $M_H = 300$ GeV and the second error reflects the change of M_W when the Higgs mass is varied between 60 and 1000 GeV.

A more precise determination of M_W will provide a stringent test of the SM. A disagreement between the value of M_W derived from the global fit and the value extracted from direct measurement would represent a major failure of the SM. Alternatively, an improvement in the value of the W mass can significantly tighten present bounds on the Higgs mass.

Two methods have been singled out as the most promising [2]. The first one is based on the rapid increase of the total cross section at threshold. The second method relies on the direct reconstruction of the mass from the hadronic decay products of the W using the decay channels

$$W^+W^- \to q\bar{q}\ell\nu \qquad (2)$$

$$W^+W^- \to q_1\bar{q}_1 q_2\bar{q}_2 \qquad (3)$$

where $\ell = e, \mu$.

Preliminary studies indicate that the direct measurement will provide a more precise determination of the W mass than the threshold method for which a smaller number of events will be available. Combin-

---

[1] E-mail: maina@to.infn.it.
[2] E-mail: pittau@psw218.psi.ch.
[3] E-mail: pizzio@to.infn.it.

ing all decay channels, an accuracy of about 35 MeV is expected from direct reconstruction, while the ultimate precision attainable at threshold is estimated to be about 100 MeV.

In WW production triple gauge-boson couplings, which play a central role in non-abelian gauge theories, appear already at tree level and can be studied in much more detail than at lower energies [3]. At LEP2 TGC's will be mainly probed using angular distributions of the W's and of their decay products. At the higher energies available at the Next Linear Collider (NLC) it will be possible in addition to study TGC's using the energy dependence of the total production cross section, since non-standard TGC's in general lead to a cross section which increases with energy and therefore eventually violates unitarity.

On-shell W-pair production is described at tree level by a set of three diagrams, labeled (e) and (f) in Fig. 1. At the lowest level of sophistication, one can attach to them the on-shell decay of the W's. In this case all one-loop electroweak and strong radiative corrections are known [4–6]. This approach is gauge invariant, but all effects of the finite width of the W and all correlations between the two decays are neglected. In order to take these features into account one can consider the set of diagrams mentioned above with off-shell W's, which decay to four fermions. In the literature the corresponding amplitude is called CC3. CC3 however is not gauge invariant. A gauge independent description of WW production requires in the unitary gauge ten (twenty) diagrams for the semileptonic channel (2) when $\ell = \mu$ (e) and eleven diagrams for the hadronic channel (3). These amplitudes are known as CC10 (CC20) and CC11, respectively. Numerically the total cross sections obtained from CC3 and CC10 or CC11 at LEP2 and NLC energies differ by a few per mill. Larger discrepancies, of the order of several per cent, are found when comparing CC3 with CC20.

In order to extract the desired information from WW production data, theoretical prediction with uncertainties smaller than those which are foreseen in the experiments are necessary. In particular this means that radiative corrections have to be under control.

In this letter we present the complete calculation of QCD corrections to CC10. In most studies they have been included "naively" with the substitution $\Gamma_W \to \Gamma_W(1 + 2\alpha_s/\pi/3)$ and multiplying the hadronic branching ratio by $(1 + \alpha_s/\pi)$. This prescription

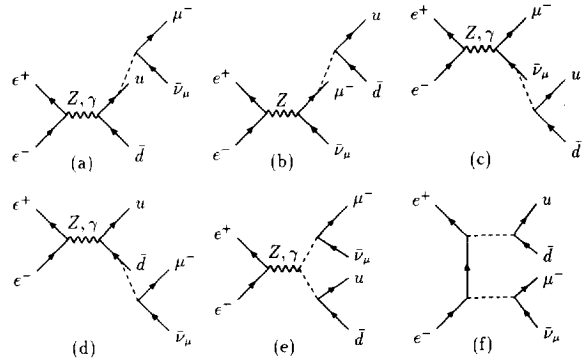Fig. 1. Tree level diagrams for $e^+e^- \to \mu^- \bar{\nu}_\mu u \bar{d}$. The dashed lines are W's.

is exact for CC3 when fully inclusive quantities are computed. However it can only be taken as an order of magnitude estimate even for CC3 in the presence of cuts on the jet directions, as discussed for the hadronic channel in [7] [4]. It is well known that differential distributions can be more sensitive to higher order corrections than total cross-sections in which virtual and real contributions tend to cancel to a large degree. It is therefore necessary to include higher order QCD effects into the predictions for WW production and decay in a way which allows to impose realistic cuts on the structure of the observed events.

2. Calculation

One-loop virtual QCD corrections to $e^+e^- \to \mu^- \bar{\nu}_\mu u \bar{d}$ are obtained by dressing all diagrams in Fig. 1 with gluon loops. Defining suitable combinations of diagrams as in Fig. 2 one can organize all contributions in a very modular way, as shown in Fig. 3. Note that the first and the fourth contributions in Fig. 3 can be obtained from each other by multiplying by -1 and interchanging momenta and helicities of u and $\bar{d}$.

The calculation has been performed using standard Passarino-Veltman techniques [9] and dimensional regularization for ultraviolet, collinear and soft divergences. With the help of the symbolic manipulation program FORM [10], all tensorial integrals have been

---

[4] The impact of QCD corrections on the angular distribution of the decay products of a W and their application to on-shell W-pair production is discussed in Ref. [8]
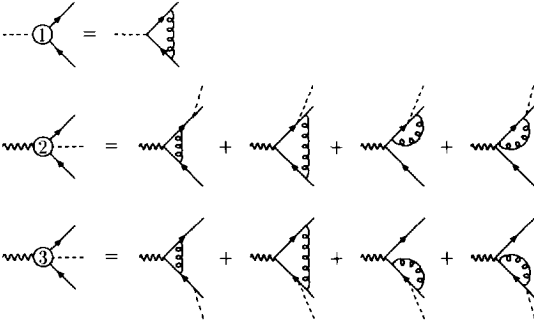
Fig. 2. Basic combinations of loop diagrams. All virtual QCD corrections to electroweak four fermion processes can be computed using these three sets. The quark wave functions corrections are not included because they vanish, in the massless limit, using dimensional regularization.
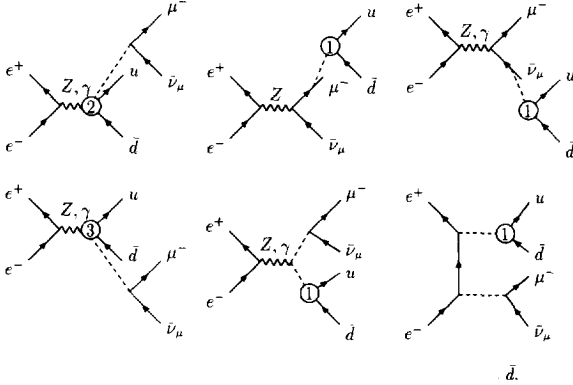

Fig. 3. One loop gluonic corrections to $e^+ e^- \rightarrow \mu^- \bar{\nu}_\mu u \bar{d}$.

reduced to linear combinations of scalar loop functions. One needs to calculate one four-point, one two-point and three three-point basic functions with different input momenta, so that twenty independent scalar loop functions contribute to the cross section.

Having classified loop corrections as in Fig. 2, one easily convinces oneself that exactly the same ingredients appear in the computation of $\mathcal{O}(\alpha_s)$ virtual corrections to any electroweak four-fermion process. In fact, due to the color structure, gluons connecting different spinor lines in the final state start contributing at $\mathcal{O}(\alpha_s^2)$. Therefore, all that is required in order to extend our results to the calculation of QCD corrections for all possible electroweak four-fermion final states is the computation of the real gluon emission amplitudes. We plan to pursue this program in the near future.

The real emission contribution for $e^+ e^- \rightarrow$

$\mu^- \bar{\nu}_\mu u \bar{d}$ can be obtained attaching a gluon to the quark line of the diagrams shown in Fig. 1 in all possible positions. This results in twenty-four diagrams. The required matrix elements have been computed using the formalism presented in Ref. [12] with the help of a set of routines (PHACT) [13] which generate the building blocks of the helicity amplitudes semi-automatically.

If we write the full NLO cross section in the form

$$\sigma_{\text{NLO}} = \int_5 d\sigma^{\text{R}} + \int_4 d\sigma^{\text{V}}, \qquad (4)$$

where we assume that all ultraviolet divergencies have been canceled by renormalization, the real (R) and virtual (V) contributions are still separately singular in four dimensions because of soft and collinear singularities, while the sum is finite.

In order to be able to integrate separately the real and virtual part one has to explicitly cancel all singular contributions in each term in a consistent way. To this aim we have used the subtraction method: the full expression (4) is rewritten in the form

$$\sigma_{\text{NLO}} = \int_5 [d\sigma^{\text{R}} - d\sigma^{\text{S}}] + \int_4 d\sigma^{\text{V}} + \int_5 d\sigma^{\text{S}}. \qquad (5)$$

The subtraction term $d\sigma^{\text{S}}$ must have the same pointwise singular behaviour as the exact real emission matrix element in order to cancel soft and collinear divergencies. It must also be possible to integrate $d\sigma^{\text{S}}$ analytically in d dimensions over the one parton subspace which generates the singularities. The result of this integration is then summed to the virtual contribution producing a finite remainder that can be treated in four dimensions. Benefits of this method are twofold. First, an exact result is obtained and no approximation needs to be taken; second, all singular terms are canceled under the integration sign and not at the end of the calculation, leading to better numerical accuracies. This is especially relevant for the present case, since we are aiming for high precision results, with errors of the order of a per mill. We have found it particularly convenient to implement the recently proposed dipole formulæ [11]. These are a set of completely general factorization expressions which interpolate smoothly between the soft eikonal factors and the collinear Altarelli-Parisi kernels in a Lorentz co-

variant way, hence avoiding any problem of double counting in the region in which partons are both soft and collinear.

All integrations have been carried out using the Monte Carlo routine VEGAS [14].

An important ingredient for accurate predictions of W-pair production is the effect of electromagnetic radiation. In the absence of a calculation of all $\mathcal{O}(\alpha)$ corrections to four-fermion processes, these effects can only be included partially. In contrast with LEP1 physics a gauge invariant separation of initial and final state radiation is not possible. On the other hand, the leading logarithmic part of initial state radiation is gauge invariant and can be included using structure functions. The non-logarithmic terms however are unknown. In order to assess the influence of QCD corrections, we are interested in a comparison with the results obtained in the Workshop on Physics at LEP2. Hence we have decided to employ as much as possible the parameters adopted in the "tuned comparisons" [15] which provide the most extensive collection of results. Therefore we have used the β prescription in the structure functions, where $\beta = \ln(s/m^2) - 1$. In the same spirit we have not included Coulomb corrections to CC3, which are known to have a sizable effect, particularly at threshold. They could however be introduced with minimal effort.

3. Results

In this section we present a number of cross sections and of distributions for $e^+ e^- \rightarrow \mu^- \bar{\nu}_\mu q_1 \overline{q_2}$. In all cases we sum over the two possibilities $(q_1, q_2) = (u, d)$ and $(q_1, q_2) = (c, s)$. The input parameters used in our calculation are given in Table 1. At LEP2 energies we have used $\alpha_s = 0.117$ as in [7], while at the NLC we have adopted $\alpha_s = 0.123$ in order to conform to the choice made for the Joint ECFA/DESY Study: Physics and Detectors for a Linear Collider. Initial state radiation is included in all results.

Previous studies [15] have shown that the differences between the total cross sections obtained from CC10 and those obtained with CC3 are at the per mill level. Much larger effects have been found in observables like the average shift of the mass reconstructed from the decay products from the true W mass. If s_- and s_+ are the invariant masses of the $\mu^- \bar{\nu}_\mu$ pair and

Table 1
Input parameters

Parameter	Value
M_Z	91.1888 GeV
Γ_Z	2.4974 GeV
M_W	80.23 GeV
Γ_W	$3 G_F M_W^3 / (\sqrt{8}\pi)$
$\alpha^{-1} = \alpha^{-1}(2M_W)$	128.07
G_F	$1.16639 \cdot 10^{-5}$ GeV^{-2}
$\sin^2 \theta_W$	$\pi \alpha(2M_W)/(\sqrt{2} G_F M_W^2)$
α_s	0.117 (0.123)
V_{CKM}	1

of the hadronic system, respectively, the standard definition is

$$\langle \Delta M \rangle = \frac{1}{\sigma} \int \left(\frac{\sqrt{s_+} + \sqrt{s_-} - 2 M_W}{2 E_b} \right) d\sigma. \qquad (6)$$

This quantity vanishes in the zero width approximation and provides a useful estimate of the influence of various physical processes on the relationship between the measured value of the W mass and its actual value.

For LEP2 we have adopted the so-called ADLO/TH set of cuts:

- $E_\mu > 1$ GeV; $10° < \theta_\mu < 170°$;
- $\theta_{\mu j} > 5°$.

Furthermore:

- the energy of a jet must be greater than 3 GeV;
- two jets are resolved if their invariant mass is larger than 5 GeV;
- jets can be detected in the whole solid angle.

For the NLC we have adopted the NLC/TH set of cuts which differs from the ADLO/TH set in that a minimum angle of 5° is required between a jet and either beam and that two jets are resolved if their invariant mass is larger than 10 GeV. Both set of cuts will also be referred to as "canonical" in the following.

The assumption that each final state particle corresponds to a jet must be abandoned when going from LO to NLO calculation. Starting from the final state partons, it is necessary to define jets using an infrared safe procedure. Only in this case the cancellation of infrared and collinear singularities between virtual and real corrections can take place and meaningful results can be obtained. In the present case it is natural to define jets using the ADLO(NLC)/TH cuts. Following these prescriptions we have merged into one jet those

Table 2
Cross sections in pb with canonical cuts (see text)

$\sqrt{s}$	Born	Exact QCD	"Naive" QCD
161 GeV	0.24962 ± 0.00002	0.24760 ± 0.00002	0.24790 ± 0.00002
175 GeV	0.96006 ± 0.00007	0.94519 ± 0.00007	0.94613 ± 0.00007
190 GeV	1.184003 ± 0.00009	1.16681 ± 0.00009	1.16766 ± 0.00008
500 GeV	0.46970 ± 0.00006	0.47109 ± 0.00007	0.46131 ± 0.00006

parton pairs whose invariant mass was smaller than 5(10) GeV. Furthermore partons with energy below 3 GeV have been merged using the JADE algorithm. Having identified jets, we have checked whether they passed the canonical cuts. All events with two or three observed jets have been retained in our plots and cross sections.

In Fig. 4 we present the normalized distribution of the angle between the muon and the closest jet at the three energies at which data will be taken at LEP2, $\sqrt{s} = 161$, 175 and 190 GeV. The corresponding cross sections are given in Table 2 together with the results at Born level and those obtained with "naive" QCD (nQCD) corrections. The events in Fig. 4 pass all ADLO/TH cuts with the exception of the minimum $\theta_{\mu j}$. Notice that imposing the latter cut corresponds to discarding only the leftmost bin in the plot. According to the ADLO/TH prescription, jets can be measured over the full solid angle. Therefore, apart from the consequences of the increase in the W width, the only possible effects of QCD radiation in the semileptonic channel are related to the increased probability of a jet to be close to the charged lepton. With increasing collider energy, the two W's tend to fly apart with larger relative momentum and therefore the probability of a jet to overlap with the lepton decreases. This behaviour is clearly visible in Fig. 4 and is confirmed by Fig. 6a which shows that at $\sqrt{s} = 500$ GeV jets are typically well separated in angle from the charged lepton and that the differences between the exact distribution and the one with "naive" corrections is confined to very large angles. From Figs. 4 and 6a it is also apparent that, as expected, exact QCD predicts smaller minimum angle between jets and the charged lepton. nQCD results for this observable become closer to the exact NLO distribution as the energy increases.

Table 2 shows that QCD corrected cross sections for $e^+e^- \rightarrow \mu^- \bar{\nu}_\mu\ q_1\ \overline{q_2}$ are between 1%, at $\sqrt{s} = 161$

GeV, to 2% smaller, at $\sqrt{s} = 190$ GeV, than Born prediction at LEP2 with ADLO/TH cuts. In the absence of cuts the exact NLO result for the total cross section and the "naive" implementation of QCD corrections agree to better than 10^{-4} and are indistinguishable within statistical integration errors for all energies studied in Table 2. This is expected since the two inclusive cross sections differ by corrections of order α_s/π to terms of relative order 10^{-3}. After cuts the two sets of results at LEP2 differ by about 10^{-3}, while statistical errors are smaller than 10^{-4}. Therefore, not surprisingly, there is clear evidence that nQCD fails even for cross sections when phase space for final particles is limited by cuts. However, with LEP2 canonical cuts the difference is much smaller than the projected experimental accuracy. Because of the additional cut on the minimum angle between jets and initial state leptons, measurements at the NLC are far less inclusive than at LEP2. The effect is further amplified by the high-energy behaviour of W-pairs which tend to be produced at smaller angles that near threshold. Therefore at $\sqrt{s} = 500$ GeV, with NLC/TH cuts, the exact NLO cross section is about 2% larger than what is obtained with nQCD, a difference which is much larger than the expected experimental uncertainties. It is amusing to note that in this case the exact NLO result is very close, about 0.5% larger, to the tree level cross section than to the nQCD prediction, which is approximately 1.5% smaller than the Born result. The decrease in cross section due to the larger width of the W is compensated by the extra radiation which leads to a larger number of events with two or more visible jets.

The mass shift $\langle \Delta M \rangle$ at $\sqrt{s} = 175$ GeV, with canonical cuts, is found to be

$$\langle \Delta M \rangle_{\mathrm{NLO}} = -0.6383 \cdot 10^{-2} \pm 0.0002 \cdot 10^{-2} \qquad (7)$$
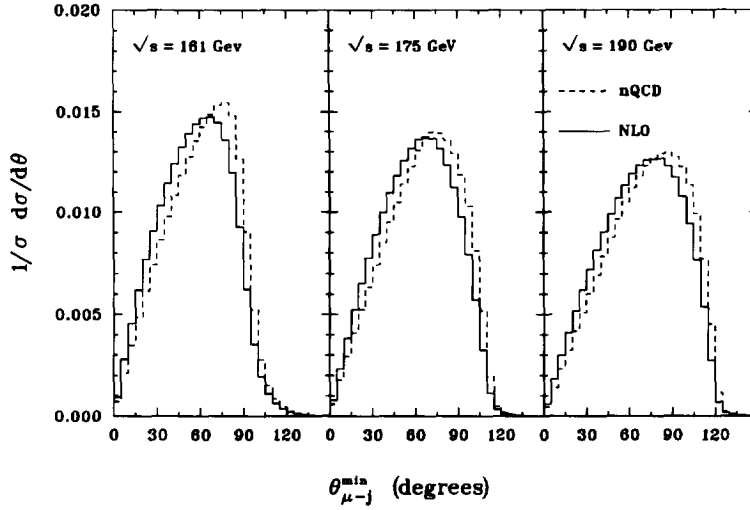
which happens to be in excellent agreement with the

Fig. 4. Distribution of the angular separation of the μ^- from the closest jet at $\sqrt{s} = 161$, 175, 190 GeV. All ADLO/TH cuts with the exception of that on $\theta_{\mu\text{-jet}}^{\min}$ are applied. The continuous histogram is the exact NLO result while the dashed histogram refers to nQCD.

nQCD result $\langle \Delta M \rangle_{\text{nQCD}} = -0.6381 \cdot 10^{-2} \pm 0.0002 \cdot 10^{-2}$. This is to be compared with the tree level result of $\langle \Delta M \rangle_{\text{Born}} = -0.6219 \cdot 10^{-2} \pm 0.0002 \cdot 10^{-2}$. Therefore the large effect, about 2.5%, of QCD corrections on $\langle \Delta M \rangle$, which was suggested by the "naive" approach [15], is confirmed by our calculation and placed on a solid footing.

Fig. 5 shows the distribution of the minimum angle between any jet and either beam at $\sqrt{s} = 175$ GeV. Even though the ADLO/TH set does not include a requirement on the θ_j angle, such a cut is included in the experimental studies for the hadronic channel, and is part of the NLC/TH set. We have separated the contribution of two-jet and three-jet final states making it possible to estimate the effect of different angular cuts on the cross section.

In Fig. 6 two distribution at $\sqrt{s} = 500$ GeV are presented. Fig. 6a shows the distribution of the angle between the muon and the closest jet, while Fig. 6b shows the distribution of the minimum angle between any jet and either beam. Fig. 6a makes it clear that essentially all events would pass any reasonable isolation cut for the μ^-. In Fig. 6b we separate again the contribution of two-jet and three-jet final states so that the effects of non-canonical cuts can be judged from the plot.
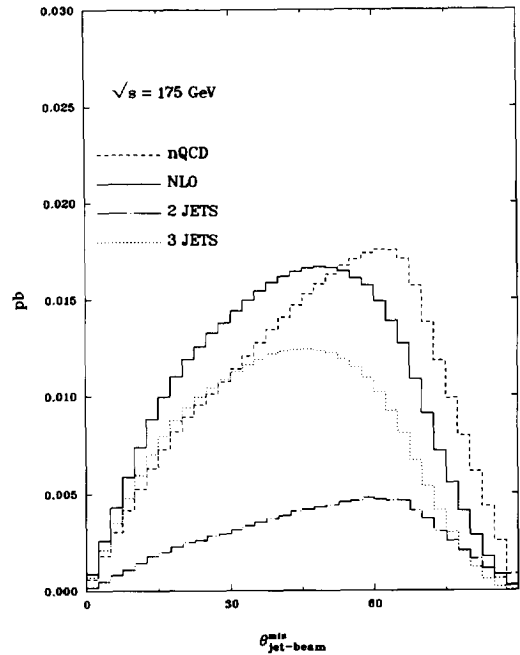

Fig. 5. Distribution of the minimum angular separation between any jet and either beam at $\sqrt{s} = 175$ GeV with canonical cuts. The continuous, dotted and dot-dashed histograms are exact NLO results while the dashed histogram refers to nQCD.
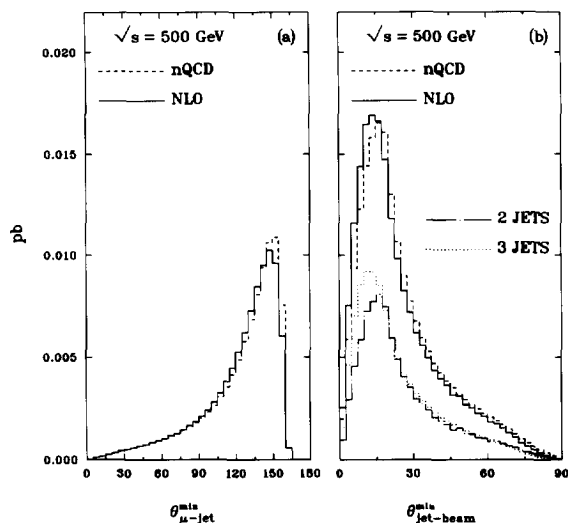
Fig. 6. Distribution of the angular separation of the μ^- from the closest jet (a) and of the minimum angular separation between any jet and either beam (b) at $\sqrt{s} = 500$ GeV. The continuous, dotted and dot-dashed histograms are exact NLO results while the dashed histogram refers to nQCD.

4. Conclusions

We have described the complete calculation of QCD radiative corrections to the semileptonic process $e^+e^- \rightarrow \mu^- \bar{\nu}_\mu u \, \bar{d}$ which are essential in order to obtain theoretical predictions for W-pair production with per mill accuracy. The amplitudes we have derived are completely differential, and realistic cuts can be imposed on the parton level structure of the observed events. It has been shown that the "naive" implementation of QCD corrections fails in the presence of cuts on the direction of final state jets. The error is typically at the per mill level at LEP2. However at $\sqrt{s} = 500$ GeV, with NLC/TH cuts, the discrepancy is about 2%, much larger than the expected

experimental precision. QCD corrections substantially increase, by more than 2%, the average shift between the W mass measured from the decay products and the actual value of M_W.

References

[1] The most complete review of W-pair production at LEP2 can be found in the Proceedings of the Workshop on Physics at LEP2, G. Altarelli, T. Sjöstrand and F. Zwirner, eds., Cern 96-01.

[2] A. Ballestrero et al., Determination of the mass of the W boson, in Ref. [1], Vol. 1, p. 141.

[3] Z. Ajaltouni et al., Triple gauge boson coupling, in Ref. [1], Vol. 1, p. 525.

[4] M. Böhm et al., Nucl. Phys. B 304 (1988) 463;
W. Beenakker, K. Kołodziej and T. Sack, Phys. Lett. B 258 (1991) 469;
W. Beenakker, F.A. Berends and T. Sack, Nucl. Phys. B 367 (1991) 287.

[5] J. Fleischer, F. Jegerlehner and M. Zrałek, Z. Phys. C 42 (1989) 409;
K. Kołodziej and M. Zrałek, Phys. Rev. D 43 (1991) 3619;
J. Fleischer, F. Jegerlehner and K. Kołodziej, Phys. Rev. D 47 (1993) 830.

[6] D. Albert, W.J. Marciano, D. Wyler and Z. Parsa, Nucl. Phys. B 166 (1980) 460.

[7] E. Maina and M. Pizzio, Phys. Lett. B 369 (1996) 341.

[8] K.J. Abraham and B. Lampe, MPI-PhT/96-14, hep-ph/9603270.

[9] G. Passarino and M. Veltman, Nucl. Phys. B 160 (1979) 151.

[10] J.A.M. Vermaseren, FORM, Computer Algebra Nederland, Amsterdam 1991.

[11] S. Catani and M.H. Seymour, preprint CERN-TH/96-29 (hep-ph/9605323).

[12] A. Ballestrero and E. Maina, Phys. Lett. B 350 (1995) 225.

[13] A. Ballestrero, in preparation.

[14] G.P. Lepage, Jour. Comp. Phys. 27 (1978) 192.

[15] E. Accomando et al., Event generators for WW physics, in Ref. [1], Vol. 2, p. 3.